Influence of the Scrape Off Layer on RF Actuator Performance

G.M. Wallace[1], I.C. Faust[1], R.J. Perkins[2], S. Shiraiwa[1], S.G. Baek[1], N. Bertelli[2], P.T. Bonoli[1], J.C. Hosea[2], R.T. Mumgaard[1], R.R. Parker[1], S.D. Scott[2], T. Shinya[3], G. Taylor[2], J.R. Wilson[2] and S.J. Wukitch[1]

[1]MIT Plasma Science and Fusion Center, Cambridge, MA, USA
[2]Princeton Plasma Physics Laboratory, Princeton, NJ, USA
[3]University of Tokyo, Tokyo, Japan

Corresponding Author: wallaceg@mit.edu

Abstract:

Experimental and modeling results from Alcator C-Mod and NSTX show that details of the scrape off layer (SOL) can significantly impact the effectiveness of radio frequency (RF) heating and current drive actuators. C-Mod experiments show that cold, dense conditions in the divertor and SOL regions ($\bar{n}_e > 10^{20}$ m^{-3}, $T_e < 20$ eV) lead to significant collisional absorption of lower hybrid (LH) waves outside the last closed flux surface (LCFS), reducing lower hybrid current drive (LHCD) efficiency in the multi-pass regime common in high density diverted experiments to date. Power flux diagnostics looking at the edge plasma show a prompt response to LH power modulation, ruling out absorption of the LH waves in the confined plasma, which would propagate out to the edge on an energy confinement timescale. The toroidally symmetric nature of the edge response indicates that the LH wave absorption is distributed around the torus outside the LCFS due to ray stochasticity in the multi-pass regime. Ray tracing/Fokker-Planck simulations including a realistic SOL model improve agreement with experimental fast electron measurements. The cold, dense regions of the SOL near the divertors strongly absorb rays through collisional absorption according to the model. Collisional damping rates calculated by a 1D full-wave model agree closely with ray tracing despite questions about the validity of the WKB approximation in the divertor/SOL regions, improving confidence in the ray tracing simulations. On NSTX, high-harmonic fast-wave power is trapped in the SOL by the righthand cutoff and thought to be dissipated in divertor RF sheaths. Electric fields in the SOL reach a maximum when the distance between the antenna and the cutoff layer is approximately one half wavelength, resulting in additional absorption outside the LCFS. These negative effects can be mitigated by moving the position of the LCFS to de-tune the resonant "cavity" formed between the antenna and the cutoff layer.

1 Introduction

Auxiliary heating and current drive (H&CD) will be necessary for sustainment and control of burning plasmas in a tokamak [1]. Radio frequency (RF) waves offer significant

advantages over neutral beams as H&CD actuators in terms of technological maturity [2], neutron streaming, and impact on tritium breeding [3, 4]. In the decades since RF heating was first observed experimentally, RF actuators have become essential components on a wide array of fusion experiments [5, 6].

Advances made in RF technology and physics have not completely overcome all difficulties. Significant hurdles remain in several areas, including (but not limited to) the survival of wave launching structures in a hostile nuclear environment [3], generation of fast particles and related modes [7], influx of impurities with metal walls [8, 9], and parasitic absorption of RF waves outside the desired damping region [10, 11, 12].

This paper will focus on the role of the scrape off layer (SOL) in parasitic absorption near or outside the last closed flux surface (LCFS). Two RF H&CD experiments, lower hybrid current drive (LHCD) on Alcator C-Mod [13] and high-harmonic fast wave (HHFW) on NSTX [14], will be used as case studies to illustrate the impact of the SOL on actuator performance.

2 Lower hybrid current drive on Alcator C-Mod

Lower hybrid (LH) current drive relies on electron Landau damping (ELD) to transfer wave energy and momentum preferentially to high-energy electrons traveling parallel to the background magnetic field [15]. The non-thermal nature of the current-carrying electrons results in a very high efficiency, $\eta \equiv n_e I_{LH} R_0 / P_{LH}$, in excess of of 3×10^{19} AW^{-1}m^{-2}. This result has been verified across a number of tokamaks at low to moderate electron density (*i.e.* $\bar{n_e} <\sim 10^{20}$ m^{-3}) [16]. This very high current drive efficiency makes LHCD a desirable tool for off-axis current drive in tokamak reactors.

The LHCD system on Alcator C-Mod operates at a source frequency, f_0, of 4.6 GHz, with 3 MW of installed source power [13]. At low to moderate density ($\bar{n}_e < 10^{20}$ m^{-3}) the LHCD system is able to drive the full plasma current (0.5-1.0 MA) with an efficiency of $2.5 - 3.5 \times 10^{19}$ AW^{-1}m^{-2}. Current drive efficiency drops precipitously as the line averaged electron density increases beyond 10^{20} m^{-3} in diverted discharges [17], however current drive is maintained beyond this threshold in limited discharges on C-Mod [18].

Prompt changes in a wide variety of SOL parameters due to the application of high power LH waves above the observed "density limit" for LHCD suggest that the LH wave power is deposited near or outside the LCFS, rather than at the mid-radius of the plasma as desired for current drive. Experiments with LHRF power modulation show an increasing fraction of the injected LHRF power as edge/SOL losses in radiative and conductive channels at timescales much faster than possible if the power is deposited in the plasma core and arrives at the edge on an energy confinement timescale [19]. Figure 1 compares the response of divertor heat flux and Lyman-α for sudden changes in ICRF and LHRF power. While the response to core-absorbed ICRF (shaded regions) occurs on the order of the energy confinement time (span between adjacent vertical dashed lines), the response to LHRF occurs much faster than an energy confinement time. Figure 2 shows the relative fractions of LH wave power that contribute to displacing Ohmic current drive, radiation from the plasma, and conduction to the divertor plates. At line averaged densities of

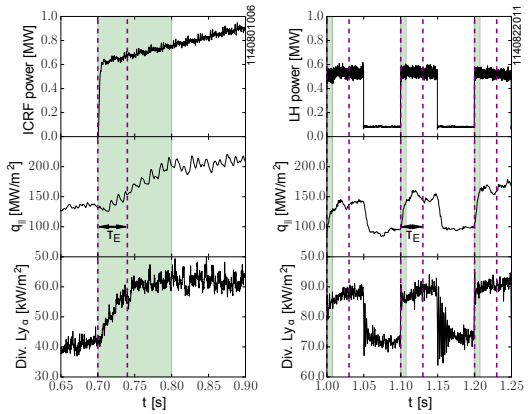

FIG. 1: (left) Response of divertor heat flux, $q_{||}$, and divertor Lyman-α emission to a sudden change in ICRF power. (right) Response of divertor heat flux and divertor Lyman-α to sudden changes in LHRF power. Reproduced from [20].

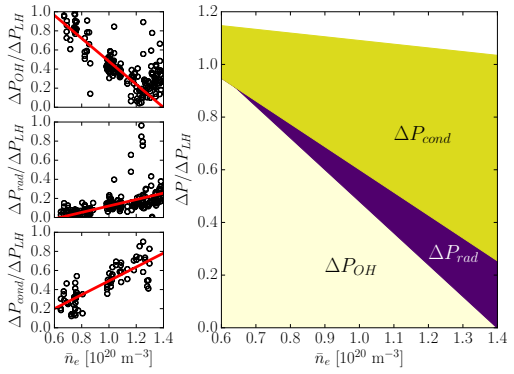

FIG. 2: Power balance of lower hybrid waves as a function of density on Alcator C-Mod. ΔP_{OH} is the change in Ohmic current drive power. ΔP_{rad} is the change in radiated power from the core and edge. ΔP_{cond} is the change in power conducted to the divertor. Reproduced from [20].

$\sim 1.4 \times 10^{20}$ m^{-3} and $I_p = 800$ kA nearly all of the injected power goes directly to the vacuum vessel wall through either conduction or radiation, the latter mainly from the region around the active divertor.

Several physical mechanisms have been proposed for the absorption of LH wave power near the LCFS. Significant upshifts in wavenumber (to $n_{||} \sim 10$) due to parametric decay instabilities (PDI) [21] and diffraction [22] could both lead to absorption of the majority of the injected power via ELD at temperatures typical of the plasma edge and SOL regions ($T_e = 20 - 500$ eV), generating a non-thermal electron tail near the edge at energies in the few keV range. Close agreement between the changes in divertor heat flux during LH power modulation experiments as measured by IR thermography with measurements based on Langmuir probes shows that the prompt change in heat flux at the divertor is thermal in nature, ruling out ELD in the edge/SOL region since any non-thermal electrons would strike the divertor before thermalizing through collisions [20]. The profile of hard X-ray bremsstrahlung generated by fast electrons remains self-consistent as density rises as shown in Figure 3, indicating that ELD does not gradually shift towards the edge at high density. Furthermore, measurements of thick-target bremsstrahlung from the strike point region are consistent with a fast electron current density in the SOL on the order of 1 A/m^2, or less than than 0.1% of the particle flux.

Toridally resolved measurements also indicate that the changes in radiated power due to LH waves are toroidally symmetric, indicating that the loss mechanism is not confined to a set of flux tubes in the SOL, but rather likely due to a process involving multiple passes of the waves through the core plasma and back into the SOL, with the stochastic nature of waves in the multi-pass regime leading to a uniform toroidal distribution.

In contrast to ELD, collisional absorption (CA) of LH waves [17] does not generate

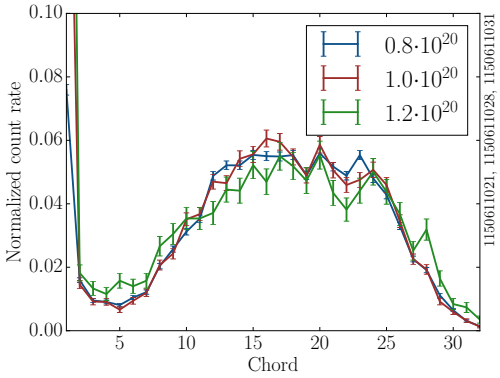

FIG. 3: Normalized hard X-ray bremsstrahlung profiles measured on Alcator C-Mod at densities below, at, and above the "density limit" are self-similar and do not show significant broadening at high density. Reproduced from [20].

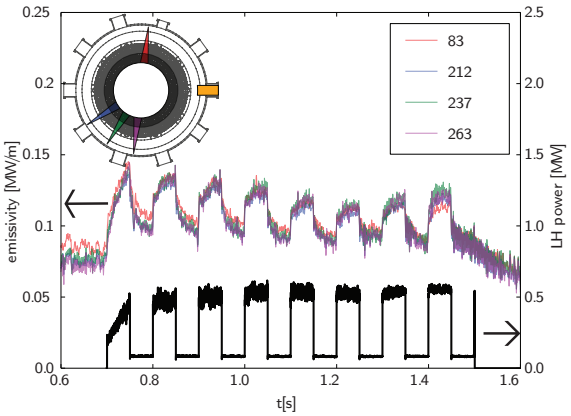

FIG. 4: Toroidally resolved bolometry measurements of radiated power during LH wave power modulation experiments. Reproduced from [19].

a non-thermal electron distribution. The GENRAY/CQL3D [23, 24] ray-tracing/Fokker-Planck code was adapted to include a fully two-dimensional SOL model to assess the impact of realistic SOL profiles on CA of LH waves. The "simple" SOL model developed in [17] shows significant CA at high density, but a discrepancy remains between the predicted and observed bremsstrahlung fluxes, particularly at the highest densities. The LHEAF/VERD full-wave/Fokker-Planck code [25] improved but did not eliminate this discrepancy. By including a two-dimensional two-point SOL model, constrained by Langmuir probes on the vacuum vessel wall and a reciprocating probe at the low field side (LFS) mid-plane, agreement between the model and experiment improves significantly across a range of plasma density and current (Figures 5 and 6) [26]. It should be noted that the simulations at high current in Figure 6 also some injected power absorbed by ELD near the LCFS, which is not verified by experiment.

Analytic calculations show that cold ($\sim$ 10 eV), dense ($\sim 10^{20}$ m^{-3}) regions of the SOL such as the divertor absorb LH wave power with e-folding lengths of $\sim$ 1 cm (Figure 7). The imaginary component of $k_\perp$ due to collisions is approximately $\omega_{pe}\nu_{ei}n_{||}/(2c\omega_0)$, where ν_{ei} is the electron-ion collision frequency. Increasing the plasma current, I_p, on C-Mod dramatically increases the LHCD effect at high density on C-Mod (Figure 6). Measurements of the 4.6 GHz wave power at locations around the tokamak also increase at higher current, suggesting that edge loss mechanisms are reduced [27, 28]. Modeling of the experiments with the "realistic" SOL model shows that the steeper density gradients in the SOL in the higher current discharges prevent the waves from propagating to the coldest regions of the SOL where collisions become the dominant absorption process. Comparisons with a one-dimensional full-wave model of CA agree closely with the analytic WKB approach, even near the cutoff density where the conditions necessary for the WKB approximation (*i.e.* $k''/k^2 << 1$) may be marginally satisfied [29]. It should be noted that

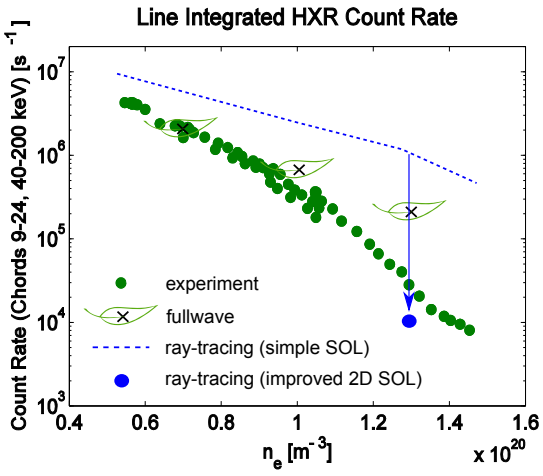

FIG. 5: Experimental hard X-ray emission as a function of density on Alcator C-Mod and model outputs from ray tracing with "simple" and "improved" SOL models, and full-wave model. Reproduced from [26].

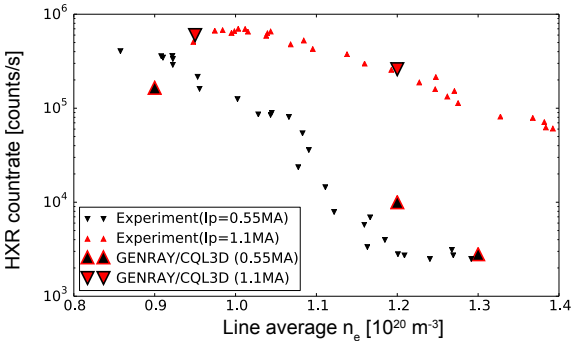

FIG. 6: Experimental hard X-ray emission as a function of density and I_p on Alcator C-Mod. Simulation results with "improved" SOL model in GENRAY indicated with large triangles. Reproduced from [26]. The results at high current show agreement with experiment at an aggregate level, but discrepancies between the radial profiles remain.

CA becomes stronger at higher $n_{||}$, so upshifts in the spectrum due to PDI or diffraction would enhance the effect of collisions.

Although LHCD experiments to date match many of the parameters of a fusion reactor (although not necessarily all at the same time), the temperature of a fusion reactor will be significantly higher. This will make single pass absorption of LH waves in a reactor very strong, reducing the impact of parasitic multi-pass losses. The LH waves will only pass through the SOL once on the way from the antenna to the LCFS, beyond which they will damp on the high temperature plasma.

3 High-harmonic fast wave on NSTX

High-harmonic fast waves on NSTX also damp parasitically in the SOL under certain conditions [31, 32, 30, 11]. Unlike the case of LHCD on C-Mod where the power loss is toroidally symmetric, the wave power deposited in the SOL on NSTX is confined to field lines passing in front of the antenna. The bright structures in Figure 8(b) transit through the SOL from in front of the HHFW antenna and spiral several times around the upper and lower divertors. Field line mappings of the spiral patterns map to the full radial width of the SOL in front of the antenna, not only at the radius of the antenna.

Langmuir probe measurements [12] and IR thermography [30] on NSTX each suggest that the heat flux beneath the spirals is strong and probably accounts for a significant fraction of the injected HHFW power. Langmuir probe $I - V$ characteristics on probes in the spiral pattern are shifted during HHFW operation relative to those not under the spiral pattern, indicating an enhancement of the sheath due to RF rectification.

Full wave simulations of the RF wave fields show that high electric fields occur in the

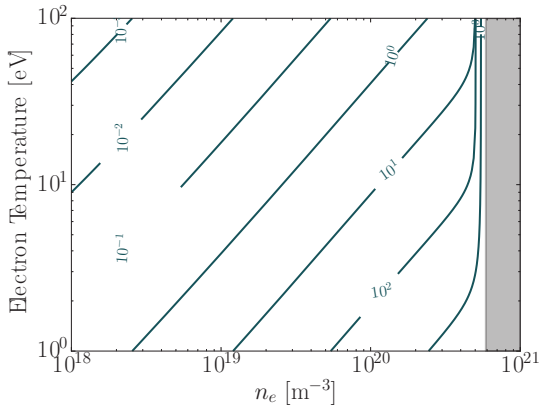

FIG. 7: Imaginary component of $k_\perp$ due to collisions for LH slow waves at 4.6 GHz, $|B| = 5.4$ T, and $n_{||} = 3$. Contour line units are in m^{-1}. Shaded region is inaccessible. Reproduced from [20].

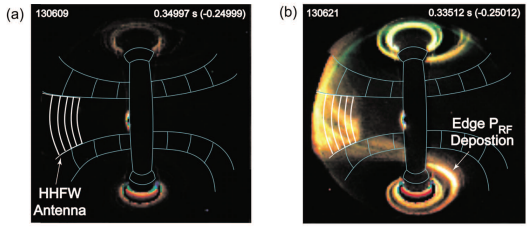

FIG. 8: Visible color camera images taken during two $I_p = 1$ MA, $B_{T0} = 0.55$ T deuterium H-mode plasmas. (a) For plasma with only 2 MW of NBI heating (shot 130609). (b) For plasma with 2 MW of NBI heating and 1.8 MW of $k_\phi = 8$ m^{-1} heating (shot 130621). Reproduced from [30].

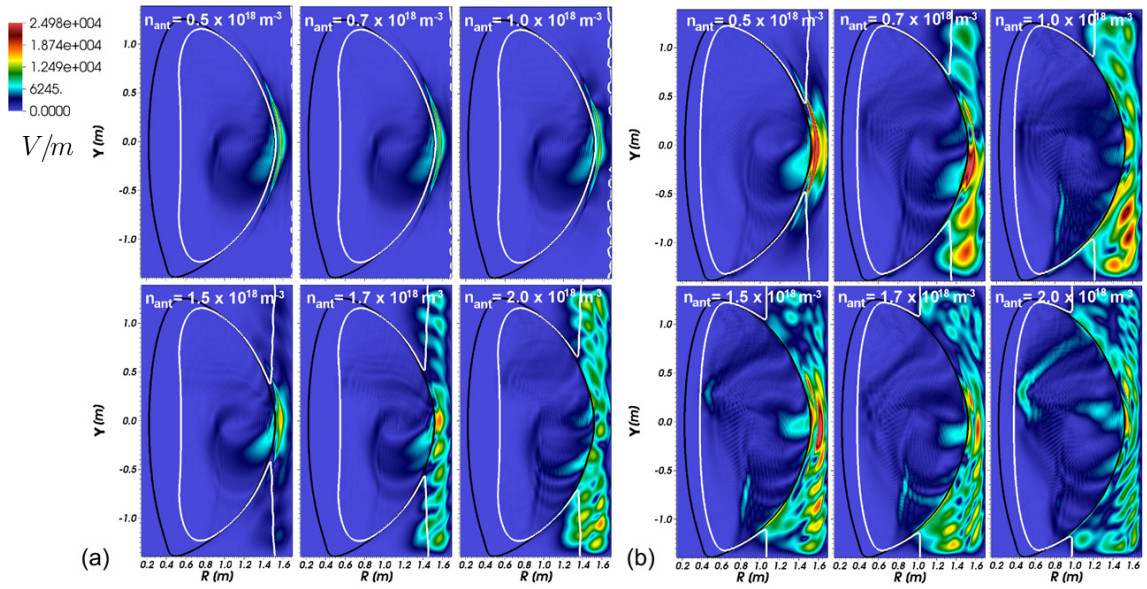

FIG. 9: Electric field amplitude for different density values in front of the antenna, n_{ant} (shown in the plots), with toroidal mode numbers $n_\phi = -21$ (a) and $n_\phi = -12$ (b). The white and black curves indicate the FW cut-off layer and the LCFS, respectively. Reproduced from [33].

SOL when the fast wave cutoff is located outside the LCFS on the low field side (Figure 9) [33]. Simulations of the fast wave in conventional aspect ratio tokamak geometry (*e.g.* C-Mod, EAST) do not exhibit the same behavior as the fast wave cutoff moves into the SOL [34].

Recent analysis in cylindrical geometry suggests that a peak in the RF standing wave may contribute to enhanced losses in the SOL when the distance between the antenna and the cutoff layer is near half a perpendicular wavelength [35]. The fast wave cutoff density ($n_{||}^2 - R = 0$, where R is the right-hand cutoff), unlike the slow wave cutoff ($\omega_{pe} = \omega_0$), is a function of $n_{||}$, frequency, and magnetic field. By varying plasma position, $n_{||}$, or magnetic field, the location of the fast wave cutoff in the SOL can be tailored to avoid these resonances, even if the fast wave is able to propagate in the SOL.

4 Discussion

Modeling of LHCD on C-Mod and HHFW on NSTX prior to the first experiments with power from the RF actuators did not anticipate the severe impact of the SOL on effective heating and current drive. Before these discoveries, the SOL was chiefly considered in the context of coupling waves out of the antenna. The cutoff layer must be in the correct proximity to the antenna for the chosen antenna type, frequency, and $k_{||}$, but beyond this little was considered about the SOL. The lesson gleaned from these two case studies is that the SOL losses must be considered as an integral part of the plasma/wave interaction in modeling of future RF experiments. Although this paper has focused on two SOL loss mechanisms (collisional absorption and RF sheath dissipation), other physical mechanisms such as parametric decay instability [36] are also sensitive to SOL parameters as well. In particular, the wide SOL envisioned for future burning plasma experiments may offset the benefits of an extremely hot plasma with high single pass absorption. Including a range of possible SOL profiles (to cover large uncertainties in profile predictions) in simulations of H&CD on these devices will be necessary to properly assess possible performance. Concurrent advances in predictive SOL profile modeling may increase confidence in the SOL profiles used in these modeling activities, although fully closing the iteration loop between between the SOL and RF models by including the effects of RF power dissipation on the SOL profile is yet to be undertaken.

Acknowledgements

This work supported by DoE Contract No. DE-FC02-99ER54512 on Alcator C-Mod, a Department of Energy Office of Science user facility, and also by DoE Contract No. DE-AC02-09CH11466 on NSTX, a Department of Energy Office of Science user facility.

References

[1] LUCE, T. C., Physics of Plasmas (1994-present) **18** (2011) 030501.

[2] MCADAMS, R., Review of Scientific Instruments **85** (2014) 02B319.
[3] WALLACE, G. M. et al., AIP Conference Proceedings **1689** (2015) 030017.
[4] SIERCHIO, J. M. et al., Bull. of the Amer. Phys. Soc. **60** (2015).
[5] ENGLAND, A. et al., Nuclear Fusion **29** (1989) 1527.
[6] KNOWLTON, S. F. et al., Nuclear Fusion **29** (1989) 1544.
[7] PINCHES, S. D. et al., Physics of Plasmas **22** (2015) 021807.
[8] WUKITCH, S. J. et al., Physics of Plasmas **20** (2013) 056117.
[9] CZARNECKA, A. et al., Journal of Nuclear Materials **463** (2015) 601 .
[10] WALLACE, G. M. et al., Physics of Plasmas **19** (2012) 062505.
[11] PERKINS, R. J. et al., Phys. Rev. Lett. **109** (2012) 045001.
[12] PERKINS, R. J. et al., Physics of Plasmas **22** (2015) 042506.
[13] BONOLI, P. T. et al., Fusion Science and Technology **51** (2007) 401.
[14] RYAN, P. et al., Fusion Engineering and Design **5657** (2001) 569 .
[15] FISCH, N. J. et al., Physical Review Letters **45** (1980) 720.
[16] BONOLI, P. T., Physics of Plasmas **21** (2014) 061508.
[17] WALLACE, G. M. et al., Physics of Plasmas **17** (2010) 082508.
[18] WALLACE, G. et al., Nuclear Fusion **51** (2011) 083032.
[19] FAUST, I. C. et al., Physics of Plasmas **23** (2016) 056115.
[20] FAUST, I., *Quantification of Lower Hybrid wave absorption in the edge of the Alcator C-Mod tokamak*, PhD thesis, Massachusetts Institute of Technology, 2016.
[21] CESARIO, R. et al., Nat. Commun. **1** (2010) 55.
[22] MENEGHINI, O., *Fullwave modeling of lower hybrid waves on Alcator C-Mod*, PhD thesis, Massachusetts Institute of Technology, 2011.
[23] SMIRNOV, A. P. et al., Bull. Am. Phys. Soc. **40** (1995) 1837.
[24] HARVEY, R. W. et al., The CQL3D Fokker-Planck Code, in *Proceedings of the IAEA Technical Committee Meeting on Simulation and Modeling of Thermonuclear Plasmas*, pages 489–526, 1992.
[25] MENEGHINI, O. et al., Physics of Plasmas **16** (2009) 090701.
[26] SHIRAIWA, S. et al., AIP Conference Proceedings **1689** (2015) 030016.
[27] BAEK, S. et al., Nuclear Fusion **55** (2015) 043009.
[28] BAEK, S. G. et al., Physics of Plasmas **23** (2016).
[29] PARKER, R. et al., Bull. of the Amer. Phys. Soc. **60** (2015).
[30] TAYLOR, G. et al., Physics of Plasmas **17** (2010) 056114.
[31] HOSEA, J. et al., Phys. Plasmas **15** (2008).
[32] HOSEA, J. C. et al., AIP Conference Proceedings **1187** (2009) 105.
[33] BERTELLI, N. et al., Nuclear Fusion **54** (2014) 083004.
[34] BERTELLI, N. et al., Nuclear Fusion **56** (2016) 016019.
[35] PERKINS, R. J. et al., Physics of Plasmas **23** (2016) 070702.
[36] PORKOLAB, M., AIP Conference Proceedings **1689** (2015) 020002.